

## **Vertical axis non-linearities in wavelength scanning interferometry**

Giuseppe Moschetti<sup>1, 2</sup>, Hussam Muhamedsalih<sup>2</sup>, Daniel O'Connor<sup>1</sup>, Xiangqian Jiang<sup>2</sup>, Richard K. Leach<sup>3</sup>

<sup>1</sup>*National Physical Laboratory, Hampton Road, Teddington, UK*

<sup>2</sup>*Centre for Precision Technologies, School of Computing and Engineering, University of Huddersfield, HD1 3DH, UK*

<sup>3</sup>*Department of Mechanical, Materials and Manufacturing Engineering, University of Nottingham, Nottingham, NG7 2RD, UK*

[Giuseppe.moschetti@npl.co.uk](mailto:Giuseppe.moschetti@npl.co.uk)

### **Abstract**

The uncertainty of measurements made on an areal surface topography instrument is directly influenced by its metrological characteristics. In this work, the vertical axis deviation from linearity of a wavelength scanning interferometer is evaluated. The vertical axis non-linearities are caused by the spectral leakage resulting from the Fourier transform algorithm for phase slope estimation. These non-linearities are simulated and the results are compared with experimental measurements. In order to reduce the observed non-linearities, a modification of the algorithm is proposed. The application of a Hamming window and the exclusion of edge points in the extracted phase are shown to increase the accuracy over the whole instrument range.

### **1 Introduction**

The raw output of an optical interferometer is typically a fringe pattern from which the phase distribution can then be extracted. The phase distribution can then be used to determine the desired parameter, such as object shape, refractive index or displacement. The method used to determine the phase can affect the measurement in terms of its accuracy and precision.

A fringe pattern is generally given by the equation

$$I(k) = a(k) + b(k) \cos[\varphi(k)] \quad (1)$$

where  $I(k)$ ,  $a(k)$ ,  $b(k)$  and  $\varphi(k)$  are the recorded intensity, background intensity, fringe amplitude and phase, respectively. To demodulate the phase information from the recorded intensity, several techniques have been developed, such as the regularized phase tracking [1], the phase-shifting [2] and the Fourier transform technique [3]. The phase tracking technique is a minimization problem in which the fringe pattern is compared with a fringe model. The main drawback for the phase tracking technique is the poor performance when the fringe pattern is sparse. The phase shifting technique is a local method and is, therefore, sensitive to noise. The Fourier transform technique, on the other hand, is more tolerant to noise since it is a global method. This technique has been widely used to demodulate the phase slope (i.e. the instantaneous frequency) from a periodic interference pattern since it was first introduced by Takeda et al. [4]. However, accurate determination of the instantaneous frequency is an important task in other fields, such as mechanical system dynamic response [5], audio signal processing [6] and electrical power system [7].

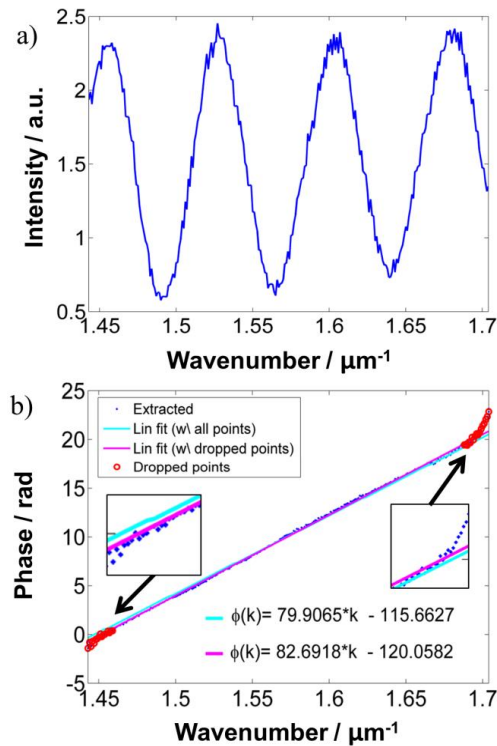


Figure 1: Fringe pattern (a) and relative demodulated and fitted phase (b). Insets show the phase deviation from linearity at the edges of the analysed windows. Equations are relative to the phase linear fitted using the entire data set of points or excluding the phase edges

The Fourier transform technique is currently used in wavelength scanning interferometry (WSI) to determine surface topography [8]. For a detailed algorithm description see Suematsu et al. [9] and Muhamedsalih et al. [10].

In this paper the effect of the Fourier transform window on the linearity of the extracted phase is investigated. The standard Fourier transform technique is modified in order to optimize the phase slope estimation and, therefore, the measurement accuracy.

The fringe pattern obtained from the WSI is described in Equation (1), the phase is given by

$$\varphi(k) = 4\pi kh \quad (2)$$

where  $h$  is the measured surface height, which is half the optical path difference (OPD) between the measurement and reference beams, and  $k$  is the wavenumber (reciprocal of wavelength) of the interfering light. In the measurement process, the wavenumber is scanned linearly and hence the phase of the fringe pattern shifts linearly with a slope proportional to the surface height. In Figure 1(a) and Figure 1(b), an example of a fringe pattern obtained from a WSI measurement is given along with the demodulated phase and linear fitting. The demodulated phase distribution deviates from its predominantly linear behaviour at the edges of the analysed window. This deviation can be explained by the phenomenon of spectral leakage, which occurs when the fringe pattern does not contain an integer number of periods [11]. Consequentially, the spectral intensity from a single frequency may not be concentrated in one bin of the Fourier transform, but instead spreads out into the surrounding bins. The width of the spectral leakage can be reduced by applying a windowing function in the Fourier transform. However, it can only be partially reduced and not entirely eliminated. To retrieve phase information, the algorithm filters out the negative frequencies in the Fourier domain. Since the spectral leakage redistributes power across the entire spectrum, information is lost through this filtering process and thus, errors are introduced in the extracted phase. These errors propagate into any parameter determined from the extracted phase. In the case of WSI this will result in an error in the phase slope estimation and therefore the measured surface topography.

## **2 Simulation**

A set of simulated fringe patterns was generated by combining Equations (1) and (2) for heights sampled in the range of 5  $\mu\text{m}$  to 35  $\mu\text{m}$ . This simulation range has been chosen to match the WSI instrument working range which is restricted to the depth of focus obtainable with a 5 $\times$  magnification objective lens. Each fringe pattern is then fed in to the Fourier transform algorithm and the height value extracted is compared with the true height to determine the error. This method was used to obtain height error as a function of the true height for different windows: Rectangular, Gaussian, Hann and Hamming (see Figure 2). Rectangular refers to the case in which the signal is Fourier transformed without window applied. For Gaussian, Hann and Hamming, the fringe pattern is

multiplied by the respective window before being Fourier transformed. For the Gaussian window, the standard deviation of the bell has been optimized to a value that gives the lowest error ( $\sigma = 73$  samples for a fringe pattern with 256 points). 256 points per fringe pattern are sampled to avoid aliasing for the expected frequencies obtainable in the working range of the instrument ( $f_s \geq 5f$ ). Note that for all cases the DC offset is removed from the fringe pattern by mean subtraction.

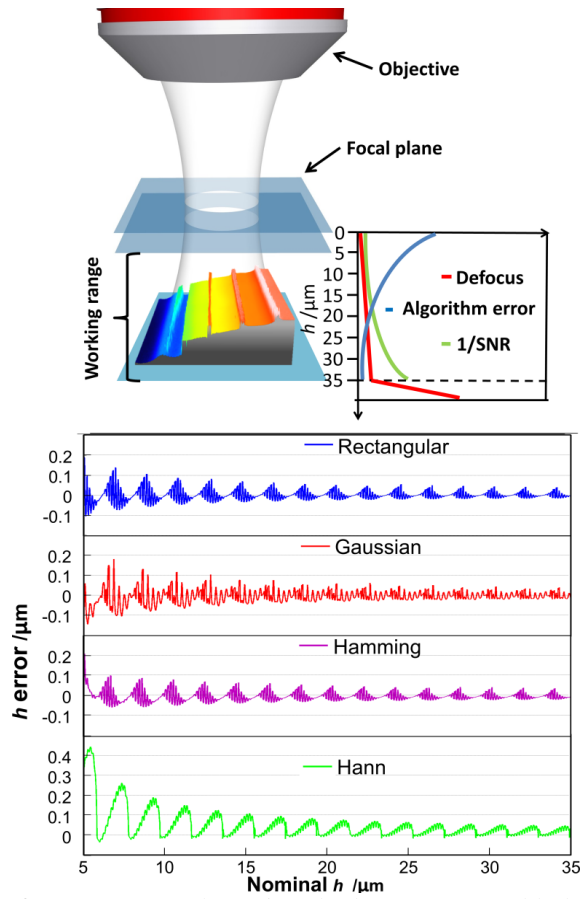


Figure 2: Left: WSI range schematic. The largest measurable height is set by both the objective depth of focus (DOF) ( $35 \mu\text{m}$  for  $5\times$ ) and signal to noise ratio (SNR); the shortest measurable height is limited by the error introduced by the algorithm. For a given accuracy only a portion of the working range can be used. Right: height error simulation results as a function of nominal height in the range  $5 \mu\text{m}$  to  $35 \mu\text{m}$ .

In each case, the height error shows an oscillatory behaviour with decreasing amplitude for larger nominal heights. Therefore for a given measurement

accuracy required, only a short portion of the instrument range can be used. The periodic zeros in the height errors correspond to points where a fringe pattern exists with an integer number of periods and thus where no spectral leakage occurs. The decreasing amplitude in error as height increases can be explained again in terms of the spectral leakage. Larger heights result in interference patterns with a larger frequency, therefore, the used frequency spectrum peak is well isolated from spectral leakage into the negative Fourier domain. Therefore less information is lost when these negative frequencies are filtered. It was found that the best performing window in the simulated range was the Rectangular function, with a maximum error of 140 nm and an RMS error of 24 nm.

By noticing that the non-linearity in the extracted phase appears to be isolated mainly to the edges of the analysed window the algorithm's performance may be improved by using only the central data of the demodulated phase to estimate the phase slope. This concept is shown in Figure 1(b). In Figure 3, the maximum and root mean square (RMS) errors against the percentage of the dropped phase points are shown for the tested windows.

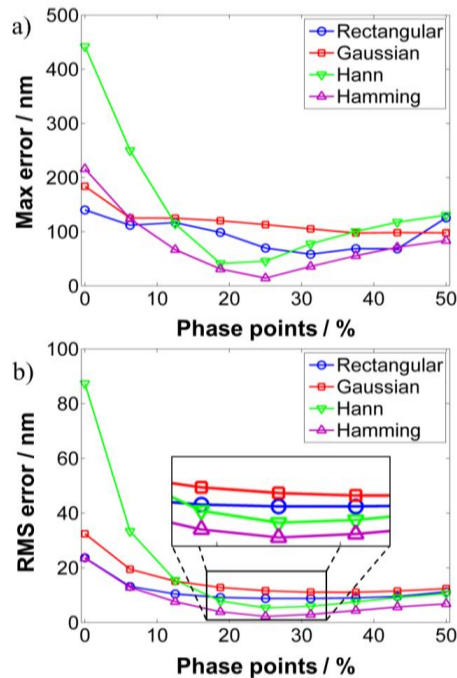


Figure 3: Maximum (a) and RMS (b) height error in the range 5  $\mu\text{m}$  to 35  $\mu\text{m}$  against percentage of dropped extremity phase points.

When more than 6.25 % of phase data were dropped, the Hamming window exhibits the lowest errors of all the windows. It has maximum and RMS errors of 14 nm and 2 nm, respectively, when 25 % of the phase points are dropped symmetrically from the phase edges, i.e. when only the central and most linear

portion of the phase is used to estimate the phase slope. This is an improvement by a factor of 10.

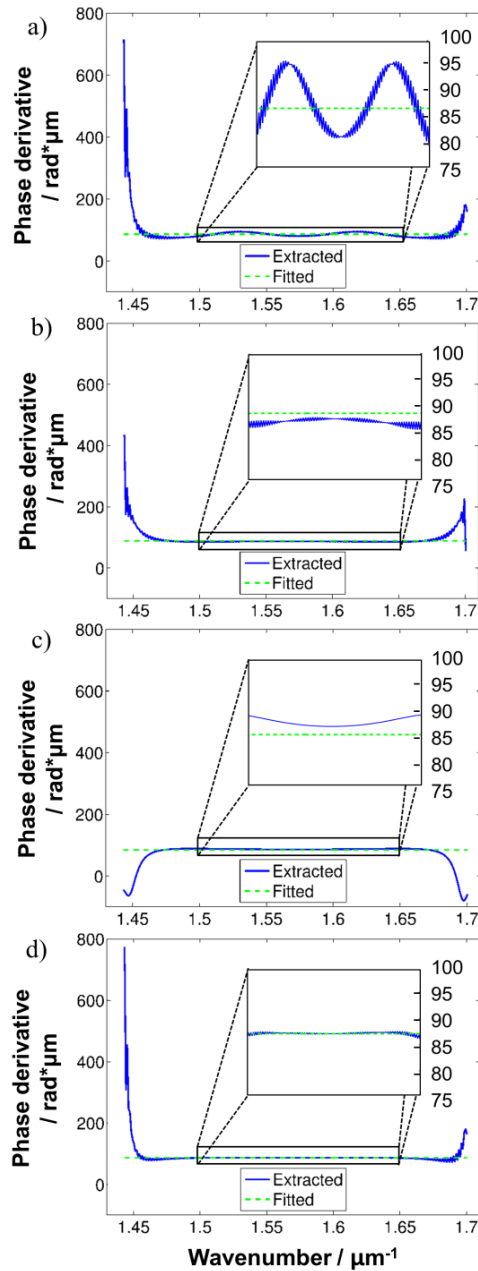


Figure 4: Comparison of the extracted phase derivative for different windows corresponding to an height of 6.9064  $\mu\text{m}$ . Rectangular(a), Gaussian (b), Hann(c), Hamming(d). The Hamming window shows the closest linear

behaviour in the central portion therefore providing the best phase derivative estimation among the tested windows.

### 3 Experimental

An optical flat surface from the NPL areal calibration set [12] was measured with the WSI to evaluate the algorithm's performance on real data. The flat was tilted to measure a continuum of different heights in the range from 5  $\mu\text{m}$  to 7  $\mu\text{m}$ , with the assumption that the response of the instrument is invariant across the field of view.

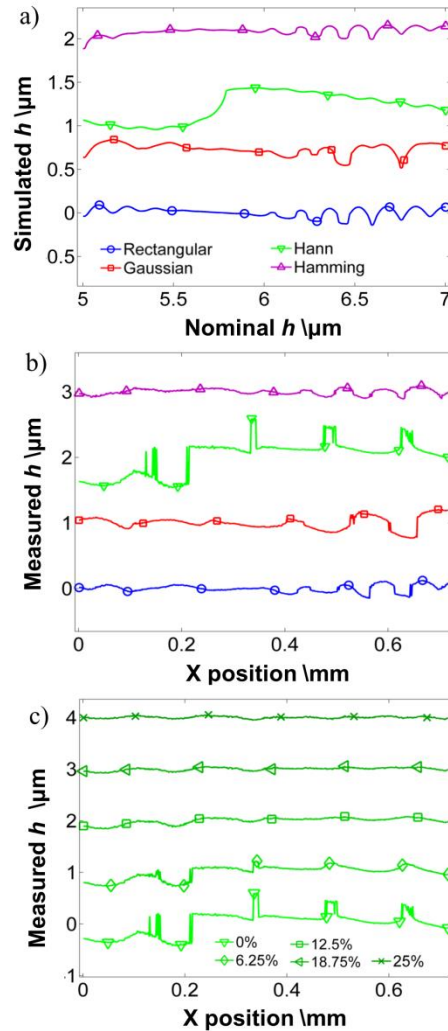


Figure 5: Simulated (a) and measured (b,c) flat profiles in the 5  $\mu\text{m}$  to 7  $\mu\text{m}$  range. Plot (a) and (b) have the same legend. Plot (c) is relative to the Hann

window case. The measured surface becomes smoother as more phase points are dropped. Note that the profiles are offset by 1  $\mu\text{m}$  and the tilt is removed for clarity reason.

The tilted optical flat was placed at this extremity of the working range since it is where the Fourier transform algorithm displays the largest errors and is practically unusable (see Figure 2). The simulated and measured profiles using different windows are in agreement and the results are shown in Figure 5(a) and Figure 5(b).

The main difference is for the Hann window, since the simulation does not show the spikes that are visible in the measurement. The origin of these spikes could be due to the noise in the real data. In Figure 5(c) the measured profiles are shown for a Hann window with an increasing percentage of dropped phase points. As the number of dropped phase points increases the surface determined by the algorithm becomes smoother, approaching the expected values for the optical flat. In order to select the optimum percentage of dropped phase points the trend in the RMS heights value,  $S_q$ , of the measured surface was evaluated. The results are shown in Figure 6.

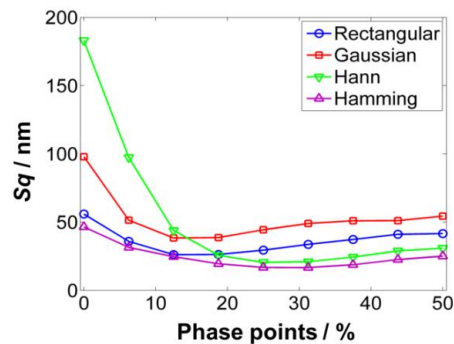


Figure 6: Measured  $S_q$  value versus percentage of discarded phase points for the optical flat surface from NPL areal calibration set.

The root mean square height value reduces when the number of discarded phase points increases. For the rectangular and the Gaussian window, a minimum value of respectively 26.2 nm and 38.4 nm is reached when 12.5 % of the phase points are discarded, with respect to the initial values of 55.9 nm and 97.9 nm. The Hann window measures the largest  $S_q$  value among the tested windows (183 nm at 0 % dropped), which drops to the minimum value of 20.5 nm when 25 % of the points are discarded. The Hamming window measures the lowest  $S_q$  value among those analysed and the measured value reaches a minimum value of 16.8 nm at 25 % from an initial value of 46.5 nm.

#### 4 Conclusion

In conclusion, the optimization of phase slope demodulation from a measured fringe pattern has been demonstrated through the application of windows in the



Fourier transform technique. Moreover, for the Hamming windows, the resulting redistribution of non-linearity in the extracted phase towards the phase edges has been exploited to determine more accurately phase slope by discarding points from the extremities before the linear fitting step. This simple optimization can be used to improve the accuracy of any measurand determined from the phase slope. In the case of WSI fringe patterns this was shown to substantially improve the accuracy of height determination thereby extending the effective working range of the instrument. This has implications for the high dynamic range challenge in metrology.

## 5 Acknowledgements

The authors gratefully acknowledge the funding of the EPSRC Centre for Innovative Manufacturing in Advanced Metrology (EP/I033424/1), ERC (ERC-ADG-228117), EU FP7 Nanomend (280581), and the NMS Engineering and Flow Programme 2011.

## 6 References

- [1] L. Kai and Q. Kema, "Improved generalized regularized phase tracker for demodulation of a single fringe pattern," *Opt. Express*, vol. **21**, no. 20, pp. 170–9, 2013.
- [2] D. Malacara, 2007, *Optical Shop Testing*. Wiley-Interscience..
- [3] Z. Malacara and M. Servín, 2005., *Interferogram Analysis For Optical Testing*. Taylor & Francis,
- [4] M. Takeda, H. Ina, and S. Kobayashi, "Fourier-transform method of fringe-pattern analysis for computer-based topography and interferometry," *J. Opt. Soc. Am.*, vol. **72**, no. 1, p. 156, 1982.
- [5] P. Frank Pai, "Online tracking of instantaneous frequency and amplitude of dynamical system response," *Mech. Syst. Signal Process.*, vol. **24**, no. 4, pp. 1007–24, 2010.
- [6] M. Grimaldi and F. Cummins, "Speaker identification using instantaneous frequencies," *IEEE Trans. audio, speech, Lang. Process.*, vol. **16**, no. 6, pp. 1097–111, 2008.
- [7] M. B. Djurić and Ž. R. Djurišić, "Frequency measurement of distorted signals using Fourier and zero crossing techniques," *Electr. Power Syst. Res.*, vol. **78**, no. 8, pp. 1407–15, 2008.
- [8] X. Jiang, K. Wang, F. Gao, and H. Muhamedsalih, "Fast surface measurement using wavelength scanning interferometry with compensation of environmental noise," *Appl. Opt.*, vol. **49**, no. 15, pp. 2903–09, 2010.
- [9] M. Suematsu and M. Takeda, "Wavelength-shift interferometry for distance measurements using the Fourier transform technique for fringe analysis.," *Appl. Opt.*, vol. **30**, no. 28, pp. 4046–55, . 1991.
- [10] H. Muhamedsalih, F. Gao, and X. Jiang, "Comparison study of algorithms and accuracy in the wavelength scanning interferometry.," *Appl. Opt.*, vol. 51, no. 36, pp. 8854–62, Dec. 2012.
- [11] J. Harris, "On then Use of Windows with the Discrete for Harmonic Analysis Fourier Transform," *Proc. IEEE*, vol. **66**, no. 1, p. 51, 1978.
- [12] "NPL Areal Calibration set," 2014. [Online]. Available: <http://www.npl.co.uk/upload/pdf/areal-calibration-set.pdf>.